High Performance of Multifunctional Cotton Fabrics Modified with TiO2, Fe, Ag-doped TiO2 and Graphene Oxide Nanomaterials towards Antimicrobial and Adsorption Removal of Methylene Blue Dye

M. Khairy (mohkhairy@fsc.bu.edu.eg)
Benha University Faculty of Science https://orcid.org/0000-0002-6343-5250
R. Kamal
Benha University Faculty of Science
M. A. Mousa
Benha University Faculty of Science

Research Article

Keywords: Nanocomposites, Cotton fabrics, Antimicrobial activity, Dye Removal, Adsorption isotherm, Kinetics

Posted Date: March 5th, 2021

DOI: https://doi.org/10.21203/rs.3.rs-274902/v1

High Performance of Multifunctional Cotton Fabrics Modified with TiO_2, Fe, Ag-doped TiO_2 and Graphene Oxide Nanomaterials towards Antimicrobial and Adsorption Removal of Methylene Blue Dye

M. Khairy [a, b,*], R. Kamal[a, c], M. A. Mousa[a]

[a]Chemistry Department, Faculty of Science, Benha University, Benha, Egypt.

[b]Chemistry Department, Faculty of Science, Imam Mohammad Ibn Saud Islamic University, Kingdom of Saudi Arabia

[c]Ministry of Trade and Industry (Industrial Control Authority), Egypt

Abstract

Multifunctional cotton textile nanocomposites are well developed by the functionalization of cotton with pure TiO_2, Ag-, Fe-doped TiO_2, and graphene oxide nanoparticles via sol-gel and modified Hummer methods. The treated fabrics materials are investigated by XRD, FT-IR, and SEM. The obtained treated fabrics have been used as an adsorbent for the methylene blue dye removal from aqueous solution. The functionalized cotton fabrics are tested for antimicrobial capability towards Escherichia coli, Bacillus cereus, and Candida albicans. All functionalized fabrics have higher antimicrobial activity compared to untreated cotton especially the fabrics containing silver and Fe doped TiO_2. The optimum conditions of the adsorption process are determined via the study of the effect of the initial concentration of dye, pH, and contact time on the removal efficiency. Langmuir, Freundlich, and Tempkin isotherms are applied for the equilibrium adsorption data. GO-Cot and Ag-Ti@GO-Cot samples showed the highest adsorption removal activity. The linear correlation coefficient (R^2) showed that the Temkin model well fitted the data of adsorption on the GO-Cot sample. The analysis of experimental data with different kinetic models showed that the pseudo-second-order kinetic model well fitted the adsorption data better than the other kinetic models of pseudo-first-order, Elovich, and the intra-particle diffusion.

Keywords: Nanocomposites; Cotton fabrics; Antimicrobial activity; Dye Removal; Adsorption isotherm; Kinetics.

* Corresponding author. Tel.: +20201270405481, +9660502508917.

E-mail address: mohkhairy@fsc.bu.edu.eg

1. Introduction

As a result of dealing with dyes and using them for many purposes, it is necessary to remove the dyes effectively as a result of their harm to living organisms and the environments owing to its toxicity and stability [1-3]. In the present time, there are quite a lot of water treatment processes used to remove the dyes, such as adsorption on different sorbents, microbiological decolorating, chemical breakdown by oxidation, and so on [4]. One of the most popular and effective processes is adsorption [5, 6]. Therefore, many adsorbent materials were used [6-8], such as activated carbon, which is one of the most important materials for adsorption due to its high surface area. But there is a problem with the inability to use it more than once. [5] Therefore, it is necessary to find other materials that are cheaper and can be used many times with high efficiency.

For woven natural fibers and fabrics, their surface can be treated during the manufacturing process to obtain many special characteristics such as antibacterial, adsorption, photocatalytic, ultraviolet protection, and flame retardant, etc [9–15]. Therefore, it is necessary to investigate the effect of adding nanoparticles and ultrastructure on their mechanical properties and other properties [16].

Nano-sized TiO_2 [15], SiO_2 [17], and ZnO [18], are a group of materials utilized for functionalization of fabrics. Amongst them, nanostructured TiO_2 and its composites, which possess excellent adsorptive and photocatalytic properties, consider as the most important materials used to remove the dyes from water. This is because of their non-toxicity, huge domain of implementation, chemical and photostability, lower price, higher efficiency, etc. [19]. Recently, several methods for synthesizing TiO_2 nanoparticles at low temperatures were developed [20]. Bozzi et al. have modified the surfaces of synthetic textile by TiO_2 at temperatures lower than 100 °C [21]. Daoud et al. have treated various textile fibers with a TiO_2 thin layer by a dip-pad–dry-cure process [22, 23]. TiO_2 coating on cotton is a gifted procedure in forming heat-sensitive materials with self-cleaning and anti-microbial properties, which can also be used to clean the environment.

The spread of microbes causes extremely hazardous diseases to humans, directly or indirectly. At present, nanomaterial-based antibacterial agents are the emerging agent against bacterial resistance owing to low to moderate cytotoxicity, realistic cost, and effective inhibition mechanism of antimicrobial. So, treating the textile fabrics with nanomaterials as antimicrobial

agents were needed to improve the quality of the fabric to resist infections associated with some bacteria that cause many diseases. Therefore, one of the most popular materials that can be used as anti-bacterial is a metal oxide and is used as an additive to obtain anti-bacterial textiles fabrics such as the TiO_2 nanomaterials which have been commonly tested for superiority in several applications [24]. The use of these compounds, such as titanium dioxide and doped TiO_2, as additives are very suitable due to photocatalytic activity and high anti-microbial efficiency (90%) [25]. The use of these materials instead of silver nanoparticles has apportioned us to appreciably lessen the cost of the antibacterial textile. However, since the antibacterial properties of titanium TiO_2 have a photo-induced nature; they are frequently unsteady in the dark [26]. Several literary foundations note the lack of pure titanium dioxide as a photocatalyst, involving the ineffective use of solar energy, as well as the e^- - h^+ pairs rapid recombination [27]. Because of these inadequacies, titanium dioxide modification has been required, such as doping with metals and nonmetals. Such modification should also assist to build the TiO_2 based nanocoatings antimicrobial in the dark, i.e. cause the antimicrobial properties of the coatings independent from the existence of UV-radiation, which cannot always be confirmed in hospital conditions.

In this work, textile fabrics of cotton were modified with graphene oxide, pure TiO_2, and doped TiO_2 with Ag^+ and Fe^{3+} ions. All fabrics were characterized by different tools such as XRD, FTIR, and SEM. The removal of methylene blue dye (MB), as a model of organic dyes, from wastewater by adsorption on fabrics was studied. The antimicrobial activity of these fabrics toward Escherichia coli (E. coli), Bacillus cereus (B. cereus), and Candida albicans (C. Albicans) was also tested.

2. Experimental

2.1. Materials:

A plain weaved cotton fabric was used as matrix material (120 g/m^2), weft density: 36 threads per cm; warp density: 83 threads per cm. All chemicals are reagent grade and used without further purification. Aniline, H_2SO_4 (98%), potassium permanganate ($KMnO_4$) (97%), sodium nitrate ($NaNO_3$) (95%), and sodium hydroxide (NaOH) were provided from ADWIC (98.5%), HCl (30%) supplied from DOP ORGANIK KIMYA SAN. VE TIC.LTD.STI, graphite (99.995%) provided from Fluka AG, H_2O_2 (50%) provided from EL SALAM for chemical industries. Titanium isopropoxide (98%), acetic acid (10%), and ethanol (98%) were provided

from EL SALAM for chemical industries. The water used during all the experiments was deionized (DI) water or distilled water.

2.2. Preparation methods

2.2.1. Preparation of graphene oxide (GO)

Graphene oxide was prepared by modified Hummers-Offerman's method [28]. Five gm of graphite powder was added to 120 ml of 98% of H_2SO_4 in an ice bath with continuous stirring and the temperature didn't exceed 20 °C. Then 2.5 gm $NaNO_3$, followed by 20 gm of $KMnO_4$ was added gradually to avoid a sudden increase in temperature. The obtained solution was stirred in the ice bath for 2 h and at 35 °C for 1 h. Then 250 ml of distilled H_2O was added gradually to the ice bath, which causes effervescence and temperature suddenly increased to 98 °C then cooled to room temperature after 10 min. Next, 50 ml of (H_2O_2) was added, leading to converting samples into oily color. The mixture was heated at 90°C for 30 min. The obtained mixture was centrifuged and washed by boiling distilled water until the mixture became neutral. The resulting powder was dried at 65 °C for 24 h to get graphene oxide (GO).

2.2.2. Preparation of TiO_2 nanoparticles

TiO_2 was prepared using the sol-gel method as the following: 2 ml of 10% acetic acid was added to 6 ml of titanium isopropoxide under vigorous stirring. Then 56 ml of ethanol was added dropwise after 5 min with vigorous stirring. The pH of the solution was adjusted to 1–2 by adding 2 ml of (36%) HCl. Then the obtained solution was strongly stirred for 45 min. The produced gel TiO_2 was used for functionalized the cotton fabrics.

2.2.3. Preparation of cotton fabric functionalized with GO

First, the cotton fabric was treated with a solution of sodium hydroxide 2% (w/v) under stirring at 80 ^oC for 5 min. A dispersion of an aqueous solution of GO nanosheet (5 mg/mL) into the cotton fabric surface was carried out by a vacuum filtration method to manufacture GO-Cotton fabric [29]. The treated fabric afterward dried at 60 ^oC for 10 min, and the produced cotton showed black color after the deposition of graphene oxide and symbolized as GO-Cot.

2.2.4. Preparation of cotton fabric functionalized with TiO_2

The Pad-dry-curve method was used for treating the surface of cotton fabrics with the obtained nanomaterials [30]. 10 cm × 5 cm of untreated cotton fabrics were washed with a nonionic surfactant (tween 80). These wetted fabrics were dipped in colloidal solutions of the prepared nanomaterials separately. Then, two bowl padding mangle was used to pad these fabric

samples for 15 min continuously. After completion of padding (then using a glass stem, distribute the material to the surface of the fabric and remove the excess) these fabrics were cured at 120 °C for 3 min. This step is repeated three times. Then the produced treated fabrics were washed with sodium lauryl sulfate solution to eliminate the excess nanoparticles. Finally, these fabrics were wholly washed 10 times with water and then dried. The fabric produced was denoted as Ti-Cot.

2.2.5. Preparation of cotton fabric functionalized with silver or Ferric doped TiO_2

Cotton fabrics were coated with TiO_2 doped with Ag^+ using the above-mentioned method for coating the fabrics with pure TiO_2. Where, 0.12 g $AgNO_3$ was added to the mixture of fabrics and TiO_2 before adding ethanol. The fabric produced was designed as Ag-Ti-Cot.

The same procedures were carried out to prepare the functionalized cotton fabrics with ferric but with using 0.578 g 0.578 g $Fe(NO_3)_3.9H_2O$. The fabric produced was denoted as Fe-Ti-Cot.

2.2.6. Preparation of GO-Cotton fabric functionalized with TiO_2

GO-Cotton fabrics were coated with TiO_2 using the above-mentioned method used for coating the fabrics with pure TiO_2. The fabric produced was denoted as Ti@ GO-Cot.

2.2.7. Preparation of GO-Cotton fabric functionalized with Ag or Fe doped TiO_2

GO/Cotton fabric was also coated with Ag-doped TiO_2 using the above-mentioned method used for coating the fabrics with pure TiO_2. Where, 0.12 g $AgNO_3$ was added to the mixture of fabrics and TiO_2 before adding ethanol. The fabric produced was symbolized as Ag-Ti@GO-Cot.

The same procedures were carried out to prepare the functionalized cotton fabrics with ferric but with using 0.578 g 0.578 g $Fe(NO_3)_3.9H_2O$. The fabric produced was denoted as a Fe-Ti@GO-Cot.

2.3. Physico-chemical characterization

Before making the characterization of the prepared coated cotton, the samples were washed several times by distilled water and dried at 60 °C for 24 h. The fabric samples were weighed before and after the treatment process. For comparing the physical properties of the coated cotton samples, a constant weight of the covering materials on the cotton surface was used.

2.3.1. X-ray diffraction (XRD)

The crystallinity and types of phases present in the samples were determined by X-ray diffraction (XRD) analysis. XRD measurements were done in the range of $2\theta = 5^{o}$ - 80^{o} on a Diano (made by Diano Corporation, U.S.A.), using Cu Kα radiation ($\lambda = 1.5406$ Å).

2.3.2. The attenuated total reflection-Fourier transform infrared Spectroscopy (ATR-FTIR)

The Fourier transform infrared (FTIR) spectra were monitored via a double beam Perkin Elmer Spectrometer coupled with an ATR unit. The spectra were recorded in the 4000–400 cm^{-1} region.

2.3.3. Scanning Electron Microscope (SEM)

Determination of morphologies of untreated and treated fabrics and the effect of functionalization of cotton with different materials was carried out by a JSM-5200 Scanning Electron Microscope (JEOL) using conductive carbon paint.

2.3.4. Adsorption of methylene blue (MB) experiments

The capability of the treated and untreated fabrics for removal of methylene blue dye (MB) by adsorption from aqueous solution was tested at 25 ºC using an equilibrium technique. The adsorption isotherm was determined as the following, a piece of fabrics of 2 × 3 cm was added to 50 ml of the known initial concentration of MB dye solution with strong stirring at 25 ºC and pH = 9. Initial dye concentrations were changed in the range of 5 ppm to 20 ppm. At different time intervals, samples were withdrawn. Using UV–vis spectrophotometer (Jasco V-550, Japan) the remaining dye concentration was measured at the suitable wavelength (400 - 800 nm) relating to the maximum absorption of MB dye ($\lambda_{max} = 664$ nm). The adsorption capacity of the adsorbent was evaluated via obtained data. The impact of different initial dye concentrations on the adsorption capacity was tested. The percentage of removal (%R) of dye in the supernatant solution is calculated using the following relation:

$$\%R = \frac{C_0 - C_t}{C_0} \times 100 \qquad (1)$$

Where C_o (mg/L) is the initial concentration of the dye solution and C_t (mg/L) is the concentration of the dye solution at time t.

The equilibrium adsorption capacities (q_e) were then obtained by using the following equation.

$$q_e = (C_0 - C_e)\frac{V}{W} \qquad (2)$$

Where q_e is the adsorption capability (adsorption of the dye per unit mass of the sample, mg/g), C_o is the initial concentration and C_e is the equilibrium concentration of the dye in the solution (mg/L) respectively, W is the amount of adsorbent (g), and V is the solution volume (L). The pH was adjusted with dilute NaOH and HCl solutions. The adsorption isotherms were examined by Langmuir, Freundlich, and Tempkin models. The kinetics of the adsorption process were tested with pseudo-first-order, pseudo-second-order, second, Elovich, and intra-particle diffusion kinetic models.

3. Results and discussion

3.1. XRD study of cotton and coated cotton fabrics

The XRD of coated cotton with graphene oxide (GO-Cot) as well as with pure titanium dioxide (Ti-Cot), doped titanium dioxide with iron (Fe-Ti-Cot), silver (Ag-Ti-Cot), and graphene oxide (Ti@GO-Cot), graphene oxide and (iron-doped titanium dioxide) (Fe-Ti@GO-Cot) and graphene oxide (silver doped Titanium dioxide) (Ag-Ti@GO-Cot) were recorded and compared with that of cotton (Cot). The results obtained are represented in Fig. 1. The XRD pattern of pure cotton fabric has main characteristic diffraction peaks at 14.5°, 16.5°, 22.4°, and 33.85° due to the characteristic diffraction planes of (1^-10), (110), (200) and (004), respectively, characterizing to cellulose I structure [31-33]. The XRD of all the treated samples exhibit similar peaks to that of uncoated cotton but with different intensities. As shown in figure 1, the peaks intensities for uncoated cotton and cotton coated graphene oxide are higher than those of other coated pieces of cotton [34]. It might be attributed to that the titanium dioxide coating on cotton screen the ray beam from spread through the surface of cotton directly [35, 36]. It is also noted the absence of any diffraction peaks characterizing for the brookite, rutile, and/or anatase TiO_2 structures on the TiO_2-coated cotton fabrics, which could be attributed to the low content of TiO_2 on the fabrics.

3.2. ATR-FTIR study of cotton and functionalized cotton fabrics

FTIR spectra were used to investigate the various functional groups present in cotton and functionalized cotton fabrics. FT-IR spectrum of cotton (Fig. 2) showed peaks attributed to cellulose structure around 1020–1200 cm^{-1}[37]. Other distinctive bands attributed to the cellulose chemical structure were the hydrogen-bonded OH stretching at 3328 cm^{-1}, the CH stretching at 2920 cm^{-1}, the asymmetrical COO- stretching at 1645 cm^{-1}, and the CH wagging at 1316

cm^{-1}[38-41]. The figure showed also a slightly weak absorbance band for cotton at ~ 1735 cm^{-1}, which could be attributed to the existence of the carboxylic ester in waxes and pectins [42].

On coating, the cotton fabrics with pure or doped TiO_2, the intensities of the peaks related to OH groups decreased compared with those of undoped fabric. Commonly, titanium oxide shows significant bonding to hydroxyl groups [43]. Thus, the hydroxyl groups are involved in the coating process. Accordingly, it enters into the coating procedures. The incorporation process can be more verified through the reduction in the intensity observed for the bands at 1101 cm^{-1} and 1154 cm^{-1}, which can be ascribed to the C–O stretching vibration of the $–CH_2OH$ group and C-O stretching bond. Furthermore, the appearance of one additional peak at 1427 cm^{-1}, may be attributed to the symmetric stretching vibration of a bidentate carboxylic group with titanium atoms [44], and another noted at 1576 cm^{-1} due to asymmetric stretching vibration. The disappearing of the slight peak at 1714 cm^{-1} recommended that several carbonyl groups occurred in the blank cotton fabric providing favorable coordination sites with Ti- atoms [45]. The FT-IR spectrum of the cotton coated with GO showed that the peaks characterizing of GO merge in the same region of titanium and cotton.

3.3. SEM study

The surface morphologies of the control cotton fabric and coated cotton fabrics were investigated by using a scanning electron microscope and the images obtained are shown in Fig. 3. It is apparent from the micrographs that the surface of pure cotton fabrics is smooth, and does not contain any contaminations. However, the images of the coated fabrics demonstrated the inductive effect of the coating materials on the fabric surface. The image of coated cotton with TiO_2 shows the non-continuous deposition of white TiO_2 particles on the cotton fabric. The white particles in the micrographs approve that titanium dioxide was effectively coated on the surface of the fabric. Fig. 3e ensures the distribution of GO nanoparticles onto the surface of the cotton fabrics. It can be also seen some aggregates of graphene oxide on the fabric. Figs. 3(f, g, h) show also white particles of GO@TiO_2 composite on the fabric surfaces.

3.4. Antimicrobial activity

To study the antimicrobial activity of the treated and untreated cotton fabrics, Gram-positive (Bacillus cereus), Gram-negative bacteria (Escherichia coli), and Fungi Candida (Candida Albicans) were used. The coated and untreated fabrics exhibited variable degrees of

antimicrobial activity against the tested microorganisms by measuring the inhibition zone as illustrated in Table 1. It can be seen that pure cotton has antimicrobial activity toward only B. cereus. On the other hand, all coated cotton samples exhibit excellent antimicrobial activity against all tested microorganisms (C. Albicans, E. coli, and B. cereus). It was also noted that the antimicrobial activity of the samples containing silver (Ag-Ti-Cot, Ag-Ti@GO-Cot,) toward B. cereus exhibits higher activity compared to other treated samples. While the Fe-Ti@GO-Cot sample shows higher activity toward E. Coli compared to other samples. The cotton textiles coated with only titanium dioxide did not exhibit any antimicrobial effect against B.cereus.

The enhanced antibacterial ability of silver containing fabrics, as shown in the obtained results, can be attributed to the existence of the silver nanoparticles. The process of killing microorganisms can take place through the silver ions that come out from the silver particles then spread into the medium neighboring the samples [46], which appear as the inhibition zone around the samples. Numerous mechanisms of the anti-microbial effect of silver ions have been suggested: (a) Ag^+ enters the membrane of cell and link to cell walls of microorganism through the interaction with the thiol groups of microorganism proteins directing to their succeeding in-activation; (b) occurrence of denaturation effect; (c) inhibition of respiration [47]. The small size of Ag-nanoparticles improving the antimicrobial effects as a result of their large surface area for contact with the microorganisms, besides potentially improved oxidation–solvation and approval rates across cell membranes into the cytosol to disrupt intra-cellular protein thiol groups [48-50].

In the case of Ag-Ti@GO-Cot (23 mm), the obtained high antimicrobial effect against B. cerust can be ascribed to the synergistic effect of Ag- nanoparticles and the GO-nanosheets. The GO- nanosheets on the cotton fabrics occupied high specific surface area and hydrophobic character, resulting in increased barrier properties to diminish the adhesion and propagation of microorganisms from attaining the surface of fabrics [51]. Furthermore, the existence of GO-nanosheets onto cotton fibers is greatly useful to the nucleation and creation of Ag- nanoparticles since they can work as the active surface to raise their distribution as well as their stability. This restricted the aggregation of nanoparticles and assisted the continuous liberation of Ag^+ and strong binding to the microbial cells.

3.5. Adsorption studies

The adsorptive elimination of methylene blue, as a model of organic dyes from aqueous solutions, on cotton fabrics coated with pure and doped titanium dioxide as well as its composite

with graphene oxide, was studied**.** The adsorption of a dye can be influenced by significant factors, such as initial dye concentration, adsorbent dose, contact time, pH, and temperature.

3.5.1. Contact time effect

Fig. 4 displays the contact time effect on the subtraction of methylene blue dye by cotton fabrics (~2 × 3 cm) coated with pure TiO_2, Ag or/and Fe doped TiO_2, GO, composite of GO with TiO_2 at pH = 9, 298 K and 5 ppm as an initial concentration of MB. The figure shows a decline in the dye concentration with time through fast adsorption at the initial stage. This may be attributed to the fact that a huge number of surface sites are presented for adsorption, besides the existence of a concentration gradient between adsorbate in the adsorbent surface and adsorbate in solution. The concentration gradients tend to grow in MB sorption at the early stages.

Fig. 4 demonstrates that the adsorption capacity of all fabrics has the following order:

GO-Cot> Ag-Ti@GO-Cot > Ag-Ti-Cot > Ti-Cot > Fe-Ti-Cot > Cot> Ti@GO-Cot > Fe-Ti@GO-Cot

The removal efficiency after 10 min of adsorption were found to be 72.5 %, 70.7%, 67.2% , 61.5%, 55.4%, 36.1%, 35.3% and 28.4% for GO-Cot, Ag-Ti@GO-Cot, Ag-Ti-Cot, Ti-Cot, Fe-Ti-Cot, Cot, Ti@GO-Cot and Fe-Ti@GO-Cot, respectively.

3.5.2. Effect of PH

The effect of pH on the adsorptive removal of methylene blue dye was tested in the acidic (pH = 3), basic (pH = 9) and neutral media (pH = 7) at dye concentration 50 mg/L in the presence of cotton fabrics (~2 × 3 cm) and temperature of 298 K. The pH of the solution was adjusted by 0.1M NaOH or 0.1M HCL solution. The results obtained are represented in Fig. 5A, which demonstrates that the adsorption capacity increases as the pH increase to attain a basic medium. So the adsorption removal was tested at three different basic pH values (9, 11, and 12.5) as illustrated in Fig. 5B. The results show that the highest value of adsorption removal of dye was attained at pH = 9.

There are two suggested mechanisms concerning the effect of pH upon the adsorption of MB on the fabrics. They are (i) the adsorbent and the dye molecule electrostatically interacted, (ii) the dye chemically reacted with the adsorbent surface. Increasing the pH of the solution means increasing the concentration of hydroxyl groups, which are adsorbed on the surface of the cotton fabrics, gaining it a negative charge, and accordingly, electrostatic bonding occurs

between the particles of the positively charged dye with the negatively charged cotton surface, which leads to an increase in the rate of adsorption [52-55].

3.5.3. Effect of the initial concentration of dye

The impact of the initial concentration of MB (5-20 mg/L) on the dye removal was studied on Cot-GO fabric (highest adsorption capacity of the studied fabrics) and the results obtained are illustrated in Fig. 6. All other parameters are kept constant. It can be noted from Fig. 7 that the adsorption capability enhances as the initial dye concentrations increases. This may be attributed to the rise in the number of adsorbate molecules opposing the accessible binding sites on the surface of the adsorbent. Also, the rise in the initial MB dye concentration amplifies the number of collisions between adsorbent and dye cations, which improves the process of sorption.

The obtained results showed that the dye was completely removed at a dye concentration of 5 mg/L in 11 min for GO-Cot fabric. While as the concentration increases above 5 mg/L the dye was not completely removed. This can be explained on the basis that at high dye concentrations, adsorption sites are saturated, which leads to a decrease in the adsorption capacity. Whereas at low concentrations there are many adsorption sites available for all the dye molecules present in the solution.

3.5.4. Equilibrium adsorption isotherm

Adsorption equilibrium is an important physical and chemical aspect to evaluate the adsorption process as an operating unit. The diffusion of a solute between the liquid and solid phases can be detected by Langmuir, Freundlich, and Temkin models [56, 57]. Assuming that the adsorbate molecules adsorbed on at definite homogeneous sites in the absorbent material and as soon as a site occupied with the dye molecule, no additional adsorption occurs at that site according to the Langmuir model [58]. Moreover, the Langmuir model of adsorption assuming a formation of a monolayer of adsorbate molecules on an adsorbent surface of the homogeneous structure, with actively equivalent adsorption sites. The intermolecular forces rapidly diminish with distance and can be managed to predict the presence of a monolayer covering the adsorbent on the outside of the absorbent.

The Langmuir equation is given by Eq. 3:

$$C_e/q_e = 1/q_{max}K_L + 1/q_{max}\,C_e \qquad (3)$$

Where q_{max} is the theoretical maximum monolayer sorption capacity (mg/g), C_e is the equilibrium concentration of dye in solution (mg/L) and K_L are empirical constants. K_L is the Langmuir adsorption constant and evaluates the affinity of the sorbent for the solute.

In the Langmuir-sort adsorption process, the dimensionless partition component R_L indicates the impact of the isotherm shape on whether adsorption is favorable or unfavorable, which is reflected as a more dependable indicator of the capacity of adsorption. R_L is given by the following Eq. 4 [59]:

$$R_L = \frac{1}{1 + K_L C_0} \qquad (4)$$

Where C_o is the initial dye concentration. The values of R_L show the states of isotherms to be either irreversible ($R_L = 0$), unfavorable ($R_L > 1$), or favorable ($0 < R_L < 1$).

The Freundlich isotherm model is an empirical equation through which adsorption is treated on heterogeneous surfaces and is not limited to forming a single layer [60]. Also, this model takes into account the different tendencies of the binding sites on the surfaces of the adsorbent with the molecules of the adsorbent material. This model assumes that highly attractive sites are firstly the occupied. The Freundlich equation is given by Eq. 5:

$$\ln q_e = \ln K_F + \left(1/n\right) \ln C_e \qquad (5)$$

Where q_e is the equilibrium sorption capacity (mg/g), and C_e is the equilibrium concentration of dye in solution (mg/L), K_F, and n are empirical constants. The values of 1/n reveal the type of isotherm to be favorable ($0 < 1/n < 1$), irreversible ($1/n = 0$), and unfavorable ($1/n > 1$) [61].

Temkin isotherm model was also utilized to analyze the adsorption data and it can be given by the following equation:[62]

$$q_e = \frac{RT}{b_T} \ln A_T + \frac{RT}{b_T} \ln C_e \qquad (6)$$

where $(RT/b_T) = B$(J/mol) is the Temkin constant related to the heat of adsorption, A_T is the equilibrium binding constant related to the maximum binding energy (L/g), b_T is the Temkin constant related to the heat of adsorption (kJ/mol), R is the universal gas constant (8.314 J/mol/K) and T is the absolute temperature (K).

Freundlich, Langmuir, and Temkin models were applied to analyze the obtained experimental adsorption data on GO-Cot fabric. Fig. 7 show the fitting data of these three models: Freundlich (log q_e vs. log C_e) plots, the Temkin (q_e vs. ln C_e) plots, and Langmuir (C_e/q_e vs. C_e) plot for adsorption of MB.

The acceptance of any model to the practical results is usually evaluated through linear regression analysis, where the R^2 is calculated, and through its value, a judgment is made on how well the model fits the results. The parameters obtained from the fitting data are given in Table 2, which shows that the most suitable model fitted the data of adsorption on the Cot-GO sample is the Temkin model due to its highest correlation coefficient value (R^2). These results are indicating the chemical adsorption process.

The adsorption mechanism can be detected from the adsorption kinetics. The adsorption process is generally organized by three diffusion stages: (1) solute transportation from the bulk solution to the adsorbent film, (2) from the adsorbent film to the surface of the adsorbent, (3) from the surface of adsorbent to the inside of materials. The overall rate of the process of adsorption is evaluated by the slowest step [62].

Usually, the step is either the second or third step, which is produced by adsorption on the surface or that leads to intra-particle diffusion during adsorption, respectively [63].

Numerous kinetic models can be employed to know the mechanism of the sorption of solute molecules onto a sorbent. In the present work, pseudo-first-order [64], pseudo-second-order [65], intraparticle diffusion [66], second-order, and Elovich models were examined to assess the kinetic mechanism which controls the adsorption process of MB dye on pure and coated cotton, fabrics. The weight of the models was confirmed by the linear equation analyses $\ln(q_e - q_t)$ vs. t, (t/q_t) vs. t, q_t vs. $t_{1/2}$, $(1/q_e\text{-}q_t)$ vs t, and ln t vs q_t, separately.

Pseudo-first order can be represented by the following form [64]:

$$\ln(q_e - q_t) = \ln q_e - k_1 t \qquad (7)$$

Where q_t and q_e are the adsorbed amounts of dye (mg/g) at time t (min) and equilibrium, individually, and k_1 (min^{-1}) is the rate constant of pseudo-first-order. The plots of $\ln(q_e - q_t)$ versus t which are presented in Fig. 8a are used to determine the values of k_1 for all samples.

When the rate of reaction depends on the quantity of solute adsorbed on the surface of the adsorbent and the quantity adsorbed at equilibrium, the pseudo-second-order reaction can be used and given by Eq. 8 [62]:

$$t/q_t = 1/k_2 q_e^2 + t/q_e \qquad (8)$$

Fig. 8b represents the fitting plots of Equation 8 ((t/q_t) vs. t). The values of q_e, k_2, and R^2 were estimated and listed in Table 3.

The second-order model can be represented by the following form:

$$1/(q_e-q_t)=1/q_e+k_2t \quad (9)$$

Where q_t and q_e are the adsorbed amounts of dye (mg/g) at time t (min) and equilibrium, individually, and k_2 (min^{-1}) is the rate constant of second order. Fig. 9a reveals the fitting plots of Eq. 9 ((1/(qe-q_t) vs. t). The values of q_e, k_2, and R^2 were estimated and listed in Table 3.

For numerous adsorption systems, Elovich's empirical adsorption model has extensive applicability. This model was constructed based on the heterogeneity energy of sites of adsorption in the form of a rectangular distribution [67]. The mathematical equation of the kinetic model of Elovich can be expressed as follows:

$$q_t = (1/\beta)\ln(\alpha\beta)+(1/\beta)\ln t \quad (10)$$

where β is the rate of initial adsorption of the Elovich equation ($mg\cdot g^{-1}\,min^{-1}$) and α is the Elovich adsorption constant ($g\cdot mg^{-1}$) [68]; it is interrelated to the energy of adsorption [69].
The linear relation of the Elovich equation was obtained if $\alpha\beta t >> t$ and that $q = q_t$ for a time $t = t_t$ and $q = 0$ at $t = 0$ [70]. If plot q_t against ln(t) (Fig. 9b) displays a straight line with a slope of (1/β) and an intercept of (1/β) ln ($\alpha\beta$) and given in Table 3 [68].

This model has been utilized by several researchers to elucidate the kinetics of adsorption of pollutants on different adsorbents. Different mechanisms such as activation of surface, its deactivation; interface phase, and diffusion in solution were explored using this model. It suffices to explain the process with greater changes in the energy of activation [71].

Through comparing the correlation coefficients (R^2) of the Pseudo–first–order, Pseudo–second–order, second-order, and the Elovich models, it was found that the Pseudo–second-order kinetic model matches the process of adsorption of all the studied materials superior to the other three. Additionally, the departure between experimental $q_{e,exp}$, and calculated $q_{e,\,cal}$ values of the Pseudo–second-order kinetic model is very low. The good fitting line of Pseudo–second–order is shown in Fig. 8b, indicating that the adsorption–determining factor of the MB elimination may be involved in the chemisorption [72].

The kinetic results of the adsorption processes of the solutions are very important in defining the rate-determining step. The rate-determining step may be either the intra-particle (pore) diffusion or the boundary layer (film) in the adsorption process. The intra-particle diffusion process is studied by the modified Weber and Morries equation as following [66]:

$$q_t = k_{dif}\sqrt{t} + C \quad (11)$$

Where k_{dif} is the rate constant of intraparticle diffusion ($mg.g^{-1}min^{1/2}$) and C is the intercept related to the thickness of the boundary layer.

If the plot of q_t versus $t^{0.5}$ according to Eq. 11, gives a straight line, then the intraparticle diffusion controls the adsorption process and if the plots give more than one straight line, then two or more steps controlled the adsorption process. As shown in Fig. 8c, the plots have one linear relationship, and C as well as k_{dif} values gained from these plots were recorded in Table 3. This reveals that the intra-particle diffusion controls the adsorption process [73].

4. Conclusion

The functionalized cotton fabrics with titanium dioxide, doped titanium dioxide with (ferric, silver), and its composite with graphene oxide well successful obtained via a simple method. All treated cotton fabrics exhibit excellent antimicrobial activity against all tested microorganisms (B. cereus, E. coli, and C. Albicans). The fabrics containing silver and Fe have higher antimicrobial activity compared to other samples. The removal of methylene blue (MB), as a model of organic dyes by adsorption on the coated fabrics, was measured. The optimum conditions were determined to be MB dye concentration (5 mg/L), Contact Time = 15 minutes, and pH = 9 and T = 298 K. GO-Cot sample exhibits the highest adsorption capacity value than other coated and uncoated cotton samples with removal efficiency 72.5% after 10 min. It shows that the most suitable model fitted the data of adsorption on the GO-Cot sample is the Temkin model due to its highest correlation coefficient value (R^2). On comparing the correlation coefficients fitting (R^2) obtained by applying five different kinetic models, it was found that the Pseudo–second-order kinetic model fits the adsorption process of all samples. The intraparticle diffusion model exhibited one straight line, which reveals that the adsorption process was controlled by intraparticle diffusion.

References

[1] M. Rafatullah, O. Sulaiman, R. Hashim , A. Ahmad, Adsorption of methylene blueon low-cost adsorbents: a review. J. Hazard. Mater 177, 70-80(2010)

[2] J. Li, J. Feng, W. Yan, Excellent adsorption and desorption characteristics of polypyrrole/TiO_2 composite for Methylene Blue. J. Appl. Surf. Sci 279, 400-408(2013)

[3] P.K. Malik , Use of activated carbon prepared from sawdust and rice-husk for adsorption of acid dyes: a case study of Yellow 36. J. Dyes Pigments 56, 239–249(2003)

[4] E. Forgacs, T. Cserháti, G. Oros, Removal of synthetic dyes from wastewaters: a review. J. Environ. Int 30, 953–971(2004)

[5] Y.Q. Wang, G.Z. Wang, H.Q. Wang, C.H. Liang, W.P. Cai, L.D. Zhang, Chemical template synthesis of micro-nanoscale magnesium silicate hollow spheres for waste-water treatment. J Chem Eur 16: 3497–3503(2010)

[6] C.K. Lee, S.S. Liu, L.C. Juang, C.C. Wang, M.D. Lyu, S.H. Hung, Application of titanate nanotubes for dyes adsorptive removal from aqueous solution. J Hazard Mater 148, 756–760(2007)

[7] W. Cheah, S. Hosseini, M.A. Khan, T.G. Chuah, T.S.Y. Choong, Acid modified carbon coated monolith for methyl orange adsorption. Chem. Eng. J. 215–216,747–754(2013)

[8] Y. Hua, T. Guo, X. Ye, Q. Li, M. Guo, H. Liu, Z. Wu, Dye adsorption by resins: effect of ionic strength on hydrophobic and electrostatic interactions. J. Chem. Eng 228, 392–397(2013)

[9] W.A. Daoud, J.H. Xin , Low temperature sol-gel processed photocatalytic titania coating. J. Sol. Gel. Sci. Technol. 29, 25–29(2004)

[10] M.E. Ureyen, A. Dogan, A.S. Koparal, Antibacterial functionalization of cotton and polyester fabrics with a finishing agent based on silver-doped calcium phosphate powders. J. Text. Res. 82, 1731–1742(2012)

[11] K.N. Bharatha, S. Basavarajappa, Flammability Characteristics of Chemical Treated Woven Natural Fabric Reinforced Phenol Formaldehyde Composites. Proc. Mater. Sci. J. 5, 1880-1886(2014)

[12] P.G. Smirniotis, B. Thirupathi, S.N.R. Inturi, Single-step synthesis of N-doped TiO_2 by flame aerosol method and the effect of synthesis parameters. J. Aerosol. Sci. Technol. 113, 1–5(2018)

[13] S. Kathirvelu, L. D'souza, B. Dhurai, UV protection finishing of textiles using ZnO nanoparticles. Indian. J Fiber. Text. Res. 34, 267–273(2009)

[14] S. Tragoonwichian, A.O. Edgar, N. Yanumet, Double coating via repeat admicellar polymerization for preparation of bifunctional cotton fabric: ultraviolet protection and water repellence. Colloids. J. Surf. A. Physico. Chem. Eng. Asp. 349, 170–175(2009)

[15] M. Montazer, S. Seifollahzadeh, Enhanced self-cleaning, antibacterial and UV protection properties of nano TiO_2 treated textile through enzymatic pretreatment. J. Photo. Chem Photo. Biol. 87, 877–883(2011)

[16] A. Thygesen, B. Madsen, A.B. Bjerre, H. Lilholt, Cellulosic fibers: effect of processing on fiber bundle strength. J. Nat Fibers 8, 161–175(2011)

[17] L.F. Hao, Q.F. An, W. Xu, Q.J. Wang, Synthesis of fluoro-containing super hydrophobic cotton fabric with washing resistant property using nano-SiO_2 sol-gel method. J. Adv. Mater. Res. 121, 23–26(2010)

[18] A. Becheri, M. Dürr, P.L. Nostro, P. Baglioni, Synthesis and characterization of zinc oxide nanoparticles: application to textiles as UV-absorbers. J. Nanoparticle. Res. 10, 679–689(2008)

[19] S.B. Chaudhari, A.A. Mandot, P.H. Patel, Effect of nano TiO_2 pretreatment on functional properties of cotton fabric. Int. J. Eng. Res. Dev. 1, 24–29(2012)

[20] X.Q. Chen, G.B. Gu, H.B. Liu, Z.N. Cao, Synthesis of Nanocrystalline TiO_2 Particles by Hydrolysis of Titanyl Organic Compounds at Low Temperature. J. Am. Ceram. Soc. 87, 1035-1039(2004)

[21] A. Bozzi , T. Yuranova , J. Kiwi , Self-cleaning of wool-polyamide and polyester textiles by TiO_2-rutile modification under daylight irradiation at ambient temperature. J. Photo Chem. Photo. Biol. Chem. 172, 27–34(2005)

[22] K.H. Qi, J.H. Xin, W.A. Daoud, C.L. Mak, Functionalizing Polyester Fiber with a Self-Cleaning Property Using Anatase TiO_2 and Low Temperature Plasma Treatment. Int. J. Appl. Ceram. Technol. 4, 554-563(2007)

[23] W.A. Daoud, J.H. Xin, Y.H. Zhang, Surface functionalization of cellulose fibers with titanium dioxide nanoparticles and their combined bactericidal activities. J. Surf. Sci. 599, 69-75(2005)

[24] X. Tang, Q. Feng, K. Liu, Y. Tan, Synthesis and characterization of a novel nano fibrous TiO_2/SiO_2 composite with enhanced photocatalytic activity. J. Mater. Lett. 183, 175–178(2016)

[25] Y. Rilda, R. Safitri, A. Agustien, N. Nazir, A. Syafiuddin, H. Nur, Enhancement of Antibacterial Capability of Cotton Textiles Coated with TiO_2– SiO_2/Chitosan Using Hydrophobization. J. Chin. Chem. Soc. 66, 594–599(2019)

[26] N.S. Serhacheva, N.V. Yashina, N.I. Prokopov, A.A. Gainanova, G.M. Kusmicheva, E.N. Domoroshina, N.V. Sadovskaya, N.A. rokudina, A.Y. Gerwald, Antibacterial properties of nanosized zinc oxides (II) and titan oxides (IV) of different nature and their nanocomposites based of polystyrene. J. Russian Nanotechnol. 11 (1–2), 91–100(2016)

[27] X. Wan, T. Wang, Y. Dong, D. He, Development and Application of TiO_2 Nanoparticles Coupled with Silver Halide. J. Nanomater. 1-5(2014)

[28] L.J. Cote, F. Kim, J. Huang , Langmuir−Blodgett Assembly of Graphite Oxide Single Layers. J. Am. Chem. Soc. 131, 1043–1049(2009)

[29] X. Tang, M. Tian, L. Qua, S. Zhu, X. Guo, G. Han, K. Sun, X. Hua, Y. Wang, X. Xu, Functionalization of cotton fabric with graphene oxide nanosheet and polyaniline for conductive and UV blocking properties. Syn. Met. 202, 82–88(2015)

[30] S.S. Kim, J.E. Park , J. Lee , Properties and antimicrobial efficacy of cellulose fiber coated with silver nanoparticles and 3-mercaptopropyl trimethoxysilane (3-MPTMS). J. Appl. Polym Sci. 11, 92261–2267(2010)

[31] J. Zhao, J. Chen, Z. Chen, Y. Zhang, D. Xia, Q. Wang, Flexible cotton fabrics/PDA/BiOBr composite photocatalyst using bioinspired polydopamine as electron transfer mediators for dye degradation and Cr(VI) reduction under visible light. Colloid. Surf. A. 593, 124623(2020)

[32] H. Yang, Q. Zhang, Y. Chen, Y. Huang, F. Yang, Z. Lu, Ultrasonic-microwave synthesis of ZnO/BiOBr functionalized cotton fabrics with antibacterial and photocatalytic properties. Carbohyd. Polym. 201, 162–171(2018)

[33] P. Zhou, J. Lv, H. Xu, X. Wang, X. Sui, Y. Zhong, B. Wang, Z. Chen, X. Feng, L. Zhang, Z. Mao, Functionalization of cotton fabric with bismuth oxyiodide nanosheets: applications for photodegrading organic pollutants, UV shielding and selfcleaning. Cellulose 26, 2873–2884(2019)

[34] S.K.M. Maarof, W. Suhaida, M.F. Achoi, M.S. Abdullah, Preparation and Characterizations Cotton Coated Titanium Dioxide, TiO_2. J. Adv. Mater. Res. 832, 739-743(2014)

[35] O.U. Nimittrakoolcha , S. Supothina, Bactericidal activity and UV-filtering property of TiO_2- based photocatalysts coated on curtain fabrics. Res .Chem. Intmed .35, 271-280(2009)

[36] K. Qi, W.A. Daoud, J.H. Xin, C.L. Mak, W. Tang, W.P. Cheung, Self Cleaning Cotton. J Mater. Chem. 16, 4567-4574(2006)

[37] J. Bouchard, M. Douek, Structural and Concentration Effects on the Diffuse Reflectance Ftir Spectra of Cellulose, Lignin and Pulp. J. Wood. Chem. Technol. 13(4), 481–499(2006)

[38]C. Chung, M. Lee, E.K. Choe, Characterization of cotton fabric scouring by FT-IR ATR spectroscopy. J Carbohyd Polym 58(4), 417–420(2004)

[39] M.J. Uddin, F. Cesano, F. Bonino, S. Bordiga, G. Spoto, D. Scarano, A. Zecchina, Photoactive TiO_2 films on cellulose fibres: synthesis and characterization. J. Photo. Chem. Photo. Biol. A. Chem. 189, 286-294(2007)

[40] J. Yuan, J. Zhang, X.P. Zang, J. Shen, S.C. Lin, Improvement of blood compatibility on cellulose membrane surface by grafting betaines. Colloids. Surf. B. Biointerfaces. 30, 147-155(2003)

[41] E. Kontturi, P.C. Thune, J.W. Niemantsverdriet, Cellulose Model Surfaces Simplified Preparation by Spin Coating and Characterization by X-ray Photoelectron Spectroscopy, Infrared Spectroscopy, and Atomic Force Microscopy. Langmuir 19, 5735-5741(2003)

[42] Q. Wang, X . Fan, W. Gao, J. Chen, Characterization of bioscoured cotton fabrics using FT-IR ATR spectroscopy and microscopy techniques. Carbohydr. Res. 341, 2170–2175(2006)

[43] W.A. Daoud, S.K. Leung, W.S. Tung, J.H. Xin, K. Cheuk, K. Qi, Self-Cleaning Keratins. J. Chem. Mater. 20, 1242-1244(2008)

[44] J.C. Yu, L.Z. Zhang, J.G. Yu, Rapid synthesis of mesoporous TiO_2 with high photocatalytic activity by ultrasound-induced agglomeration. New. J. Chem. 26, 416-420(2002)

[45] D. Wu, M. Long, J. Zhou, W. Cai, X. Zhu, C. Chen, Y. Wu, Synthesis and characterization of self-cleaning cotton fabrics modified by TiO_2 through a facile approach. J. Surf. Coat. Technol. 203, 3728-3733(2009)

[46] B. Tomšicˇ, B. Simoncˇicˇ, B. Orel, M. Zeˇrjav, H. Schroers, A. Simoncˇicˇ, Z. Samardzija, Antimicrobial activity of AgCl embedded in a silica matrix on cotton fabric. J. Carbohydr. Polym. 75(4), 618-626(2009)

[47]V. Sedlarik, T. Galya, J. Sedlarikova, P. Valasek, P. Saha, The effect of preparation temperature on the mechanical and antibacterial properties of poly(vinyl alcohol)/silver nitrate films. J. Polym. Degrad. Stab. 95, 399–404(2010)

[48] Q.L. Feng, J. Wu, G.Q. Chen, F.Z. Cui, T.N. Kim, J.O. Kim, A mechanistic study of the antibacterial effect of silver ions on Escherichia coli and Staphylococcus aureus. J. Biomed. Mater. Res. 52, 662–668(2000)

[49] A. Panáček, L. Kvítek, R. Prucek, M. Kolář, R. Večeřová, N. Pizúrova, V.K. Sharma, T. Nevìčna, R. Zbořil, Silver colloid nanoparticles: synthesis, characterization, and their antibacterial activity. J. Phys. Chem. B.110, 16248–16253(2006)

[50] K. Kulthong, S. Srisung, K. Boonpavanitchaku, W. Kangwansupamonkon, R. Maniratanachote, Determination of silver nanoparticle release from antibacterial fabrics into artificial sweat. J. Particle. Fibre. Toxicol. 7:8(2010). DOI: 10.1186/1743-8977-7-8

[51] B. Ouadil, O. Amadine, Y. Essamlali, O. Cherkaoui, M. Zahouily, A new route for the preparation of hydrophobic and antibacterial textiles fabrics using Ag-loaded graphene nanocomposite. Colloid. Surface. A. 579: 123713(2019)

[52] R. Han, Y. Wang, P. Han, J. Shi, J. Yang,Y. Lu, Removal of methylene blue from aqueous solution by chaff in batch mode. J Hazard. Mater. 37(1), 550–557(2006)

[53] E.N. El Qada, S.J. Allen, G.M. Walker, Adsorption of methylene blue onto activated carbon produced from steam activated bituminous coal: a study of equilibrium adsorption isotherm. J. Chem. Eng. 124(1), 103–110(2006)

[54]H. Chen, J. Zhao, G. Dai, Silkworm exuviae--a new non-conventional and low-cost adsorbent for removal of methylene blue from aqueous solutions. J. Hazard. Mater. 186 (2-3), 1320–1327(2011)

[55] S. Karagoz, T. Tay, S. Ucar, M. Erdem, Activated carbons from waste biomass by sulfuric acid activation and their use on methylene blue adsorption. Bioresour. Technol. 99(14), 6214–6222(2008)

[56] I. Langmuir, The adsorption of gases on plane surfaces of glass, mica and platinum. J. Am Chem. Soc. 40, 1361–1403(1918)

[57] H.M.F. Freundlich, Over the adsorption in solution. J. Phys. Chem. 57, 385-470(1906)

[58] A.M. Donia, A.A. Atia, W.A. Al-amrani, A.M. El-Nahas, Effect of structural properties of acid dyes on their adsorption behaviour from aqueous solutions by amine modified silica. J. Hazardous. Mater. 161, 1544–1550(2009)

[59]B.A. Shah, A.V. Shah, A.J. Navik, Microwave-promoted M-PFR resin: kinetics, isotherms and sequestration of Cr(III) and Pb(II) from environmental samples. J. Iran. Poly. 21, 569-582(2012)

[60] Z. Derakhshan, M.A. Baghapour, M. Ranjbar, M. Faramarzian, Adsorption of Methylene Blue Dye from Aqueous Solutions by Modified Pumice Stone: Kinetics and Equilibrium Studies, Health. Scope. 2(3), 136–44(2013)

[61] H. Zhang, Y. Tang, D. Cai, X. Liu, X. Wang, Q. Huang, Z. Yu, Hexavalent chromium removal from aqueous solution by algal bloom residue derived activated carbon: equilibrium and kinetic studies. J. Hazard. Mater. 181, 801–808(2010)

[62] Y.S. Ho, J.C.Y. Ng, G. McKay, Kinetics of pollutant sorption by bio sorbents: Review. Sep. Purif. Methods. 29, 189-232(2000)

[63] D.D. Kavak, S. Ülkü, Kinetic and equilibrium studies of adsorption of β-glucuronidase byclinoptilolite-rich minerals. Proc. Biochem. 50, 221–229(2015)

[64] M. Roosta, M. Ghaedi, A. Daneshfar, R. Sahraei, Experimental design based response surface methodology optimization of ultrasonic assisted adsorption of safaranino by tin sulfide nanoparticle loaded on activated carbon. J. Spectrochim. Acta. A. 122, 223–231(2014)

[65] M. Saad, H. Tahir, J. Khan, U. Hameed, A. Saud, (Synthesis of polyaniline nano-particles and their application for the removal of Crystal Violet dye by ultrasonicated adsorption process based on Response Surface Methodology. J. Ultrasonics. Sonochem. 34, 600-608(2017)

[66] V. Srivastava, Y.C. Sharma, M. Sillanpää, Response surface methodological approach for the optimization of adsorption process in the removal of Cr(VI) ions by $Cu_2(OH)_2CO_3$ nanoparticles. J. Appl. Surf. Sci. 326, 257-270(2015)

[67] M. Baghdadi, UT (University of Tehran) isotherm as a novel and useful adsorption isotherm for investigation of adsorptive removal of pollutants. J. Environ. Chem. Eng. 5, 1906–1919(2017)

[68] H.I. Inyang, A. Onwawoma, A, S. Bae, The Elovich equation as a predictor of lead and cadmium sorption rates on contaminant barrier minerals. Soil. Till. Res. 155, 124–132(2016)

[69] C. Rill, Z.I. Kolar, G. Kickelbick, H.T. Wolterbeek, J.A. Peters, Kinetics and thermodynamics of adsorption on hydroxyapatite of the [160Tb] terbium complexes of the bone-targeting ligands DOTP and BPPED. Langmuir 25, 2294–2301(2009)

[70] H. Uslu, S. Majumder, Adsorption studies of lactic acid by polymeric adsorbent amberlite XAD-7: equilibrium and kinetics. J. Chem. Eng. Data. 62, 1501–1506(2017)

[71] H. Zhang, Y. Wang, P. Bai, X. Guo, X. Ni, "Adsorptive separation of acetic acid from dilute aqueous solutions: adsorption kinetic, isotherms, and thermodynamic studies. J. Chem. Eng. Data. 61, 213–219(2015)

[72] Z. Wu, X. Yuan, H. Zhong, H. Wang, G. Zeng, X. Chen, H. Wang, L. Zhang, J. Shao, Enhanced adsorptive removal of p-nitrophenol from water by aluminum metal–organic framework/reduced graphene oxide composite Intraparticle diffusion model was also used to analyze the kinetic. J. Sci. Rep. 6, 25638(2016)

[73] T. Sheela, Y.A. Nayaka, R. Viswanatha, S. Basavanna, T.G. Venkatesha, Kinetics and thermodynamics studies on the adsorption of Zn(II), Cd(II) and Hg (II) from aqueous solution using zinc oxide nanoparticles. J Powder Techno 217, 163–170(2012)

Figures

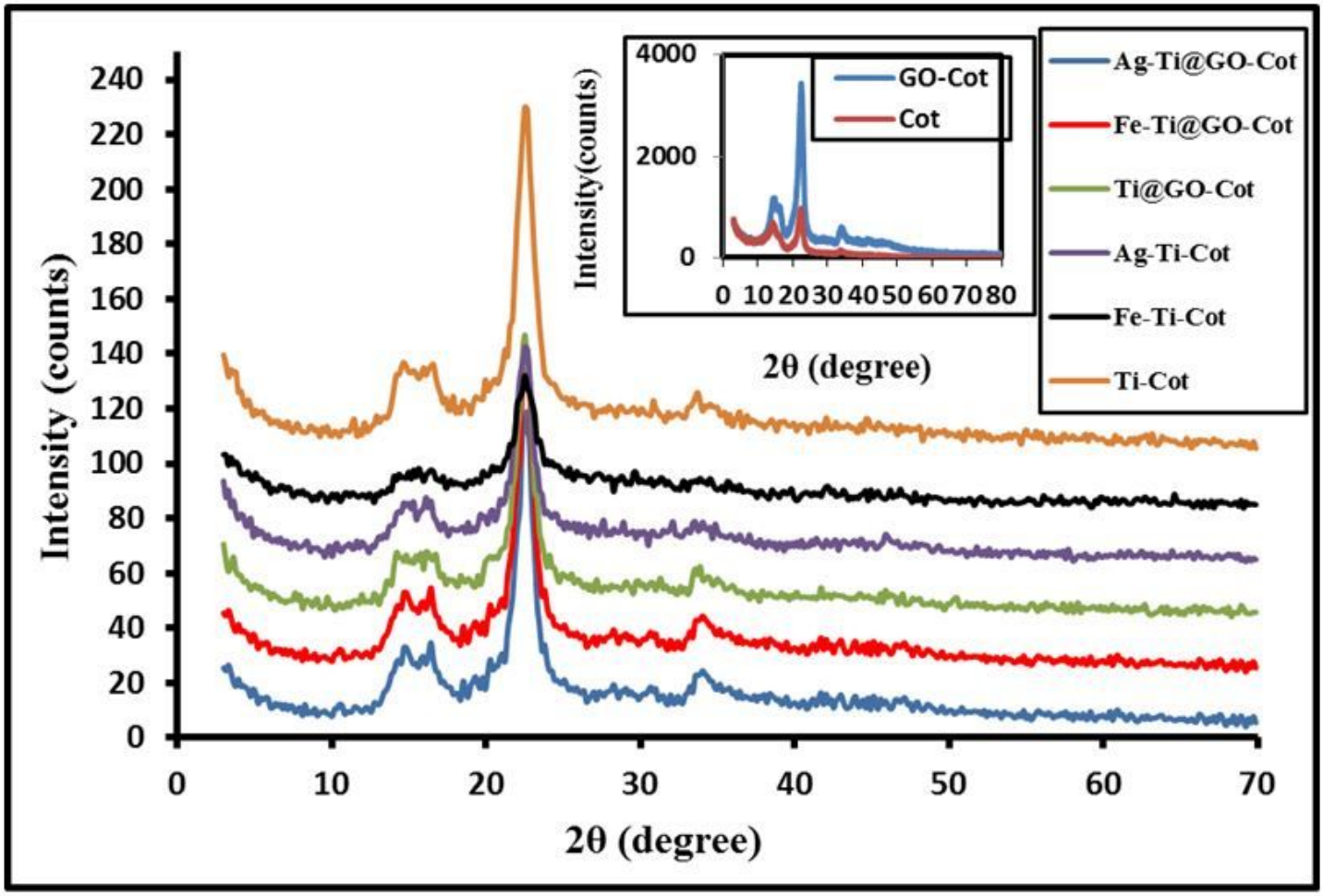

Figure 1

XRD pattern of uncoated and coated cotton fabrics.

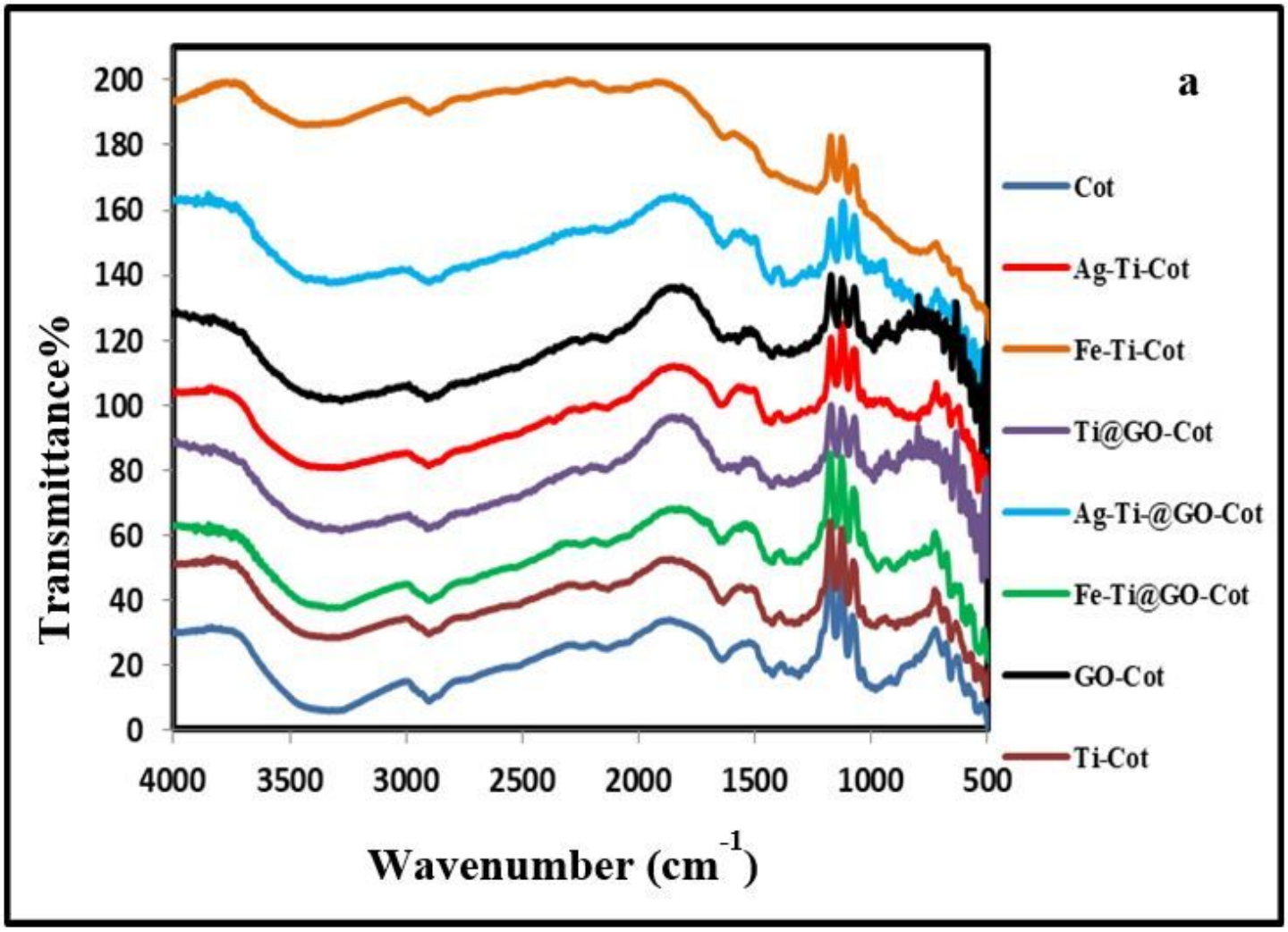

Figure 2

FTIR spectra of uncoated and coated cotton fabrics.

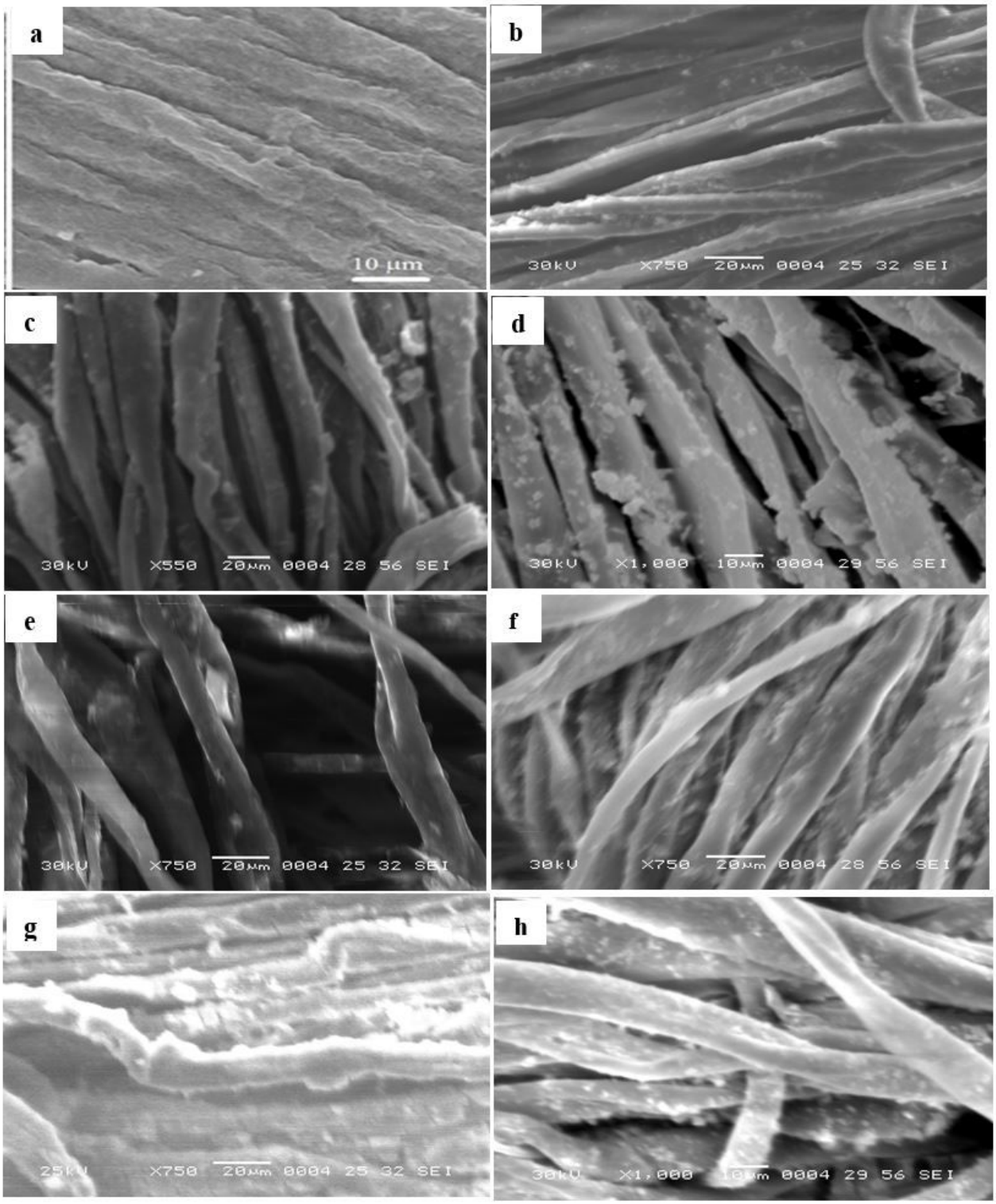

Figure 3

SEM images of cotton samples: a) Cot b) Ti-Cot c) Ag-Ti-Cot d) Fe -Ti-Cot e) GO-Cot f) Ti@GO-Cot g) Ag-Ti@GO-Cot h) Fe-Ti@ GO-Cot.

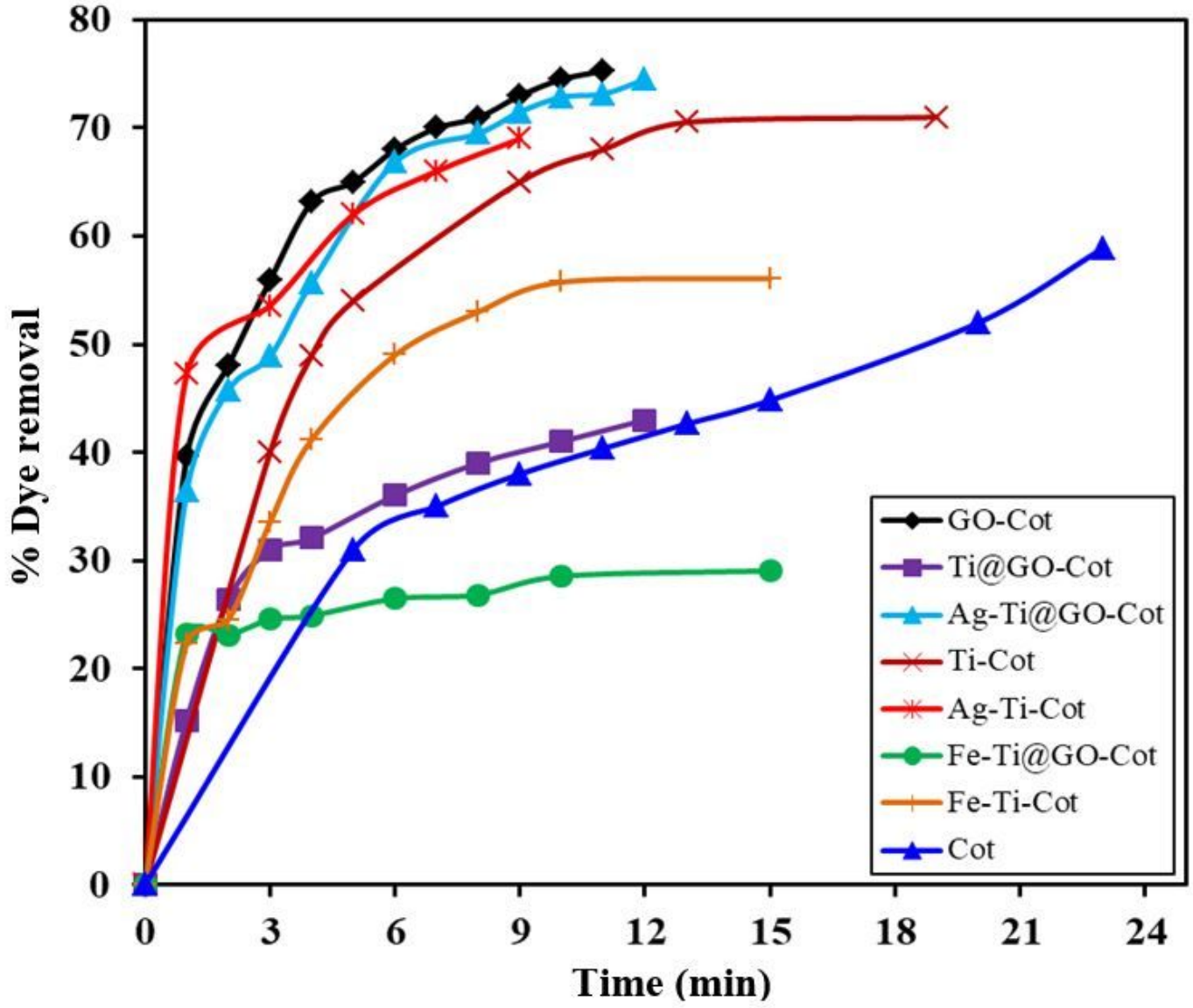

Figure 4

Effect of contact time on adsorption capacity of the investigated cotton fabrics.

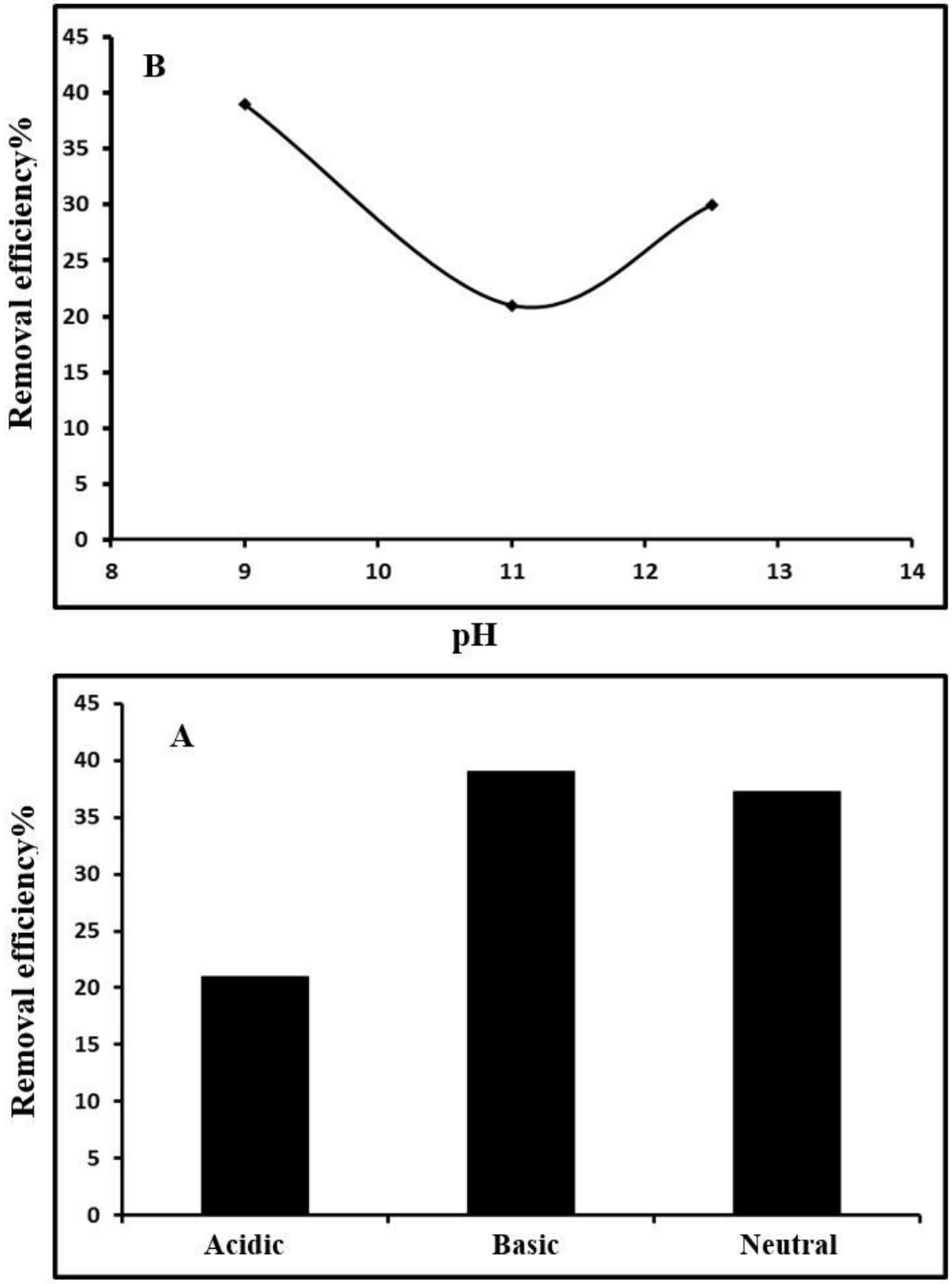

Figure 5

A) The removal efficiency of MB dye on cotton sample in different media. B) Effect of pH on the removal efficiency of MB dye on cotton sample.

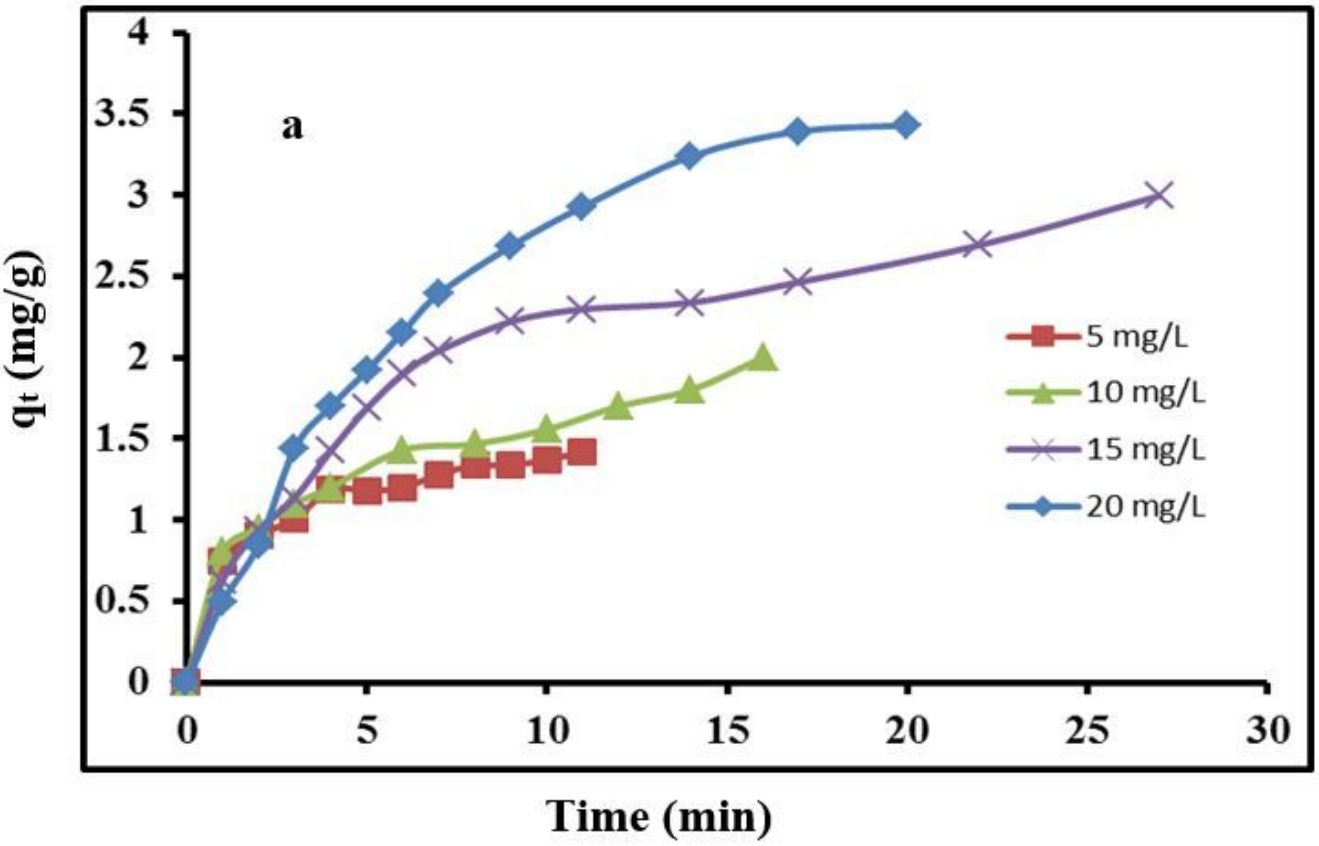

Figure 6

Effect of initial dye concentration on the adsorption of MB by: a) GO-Cot.

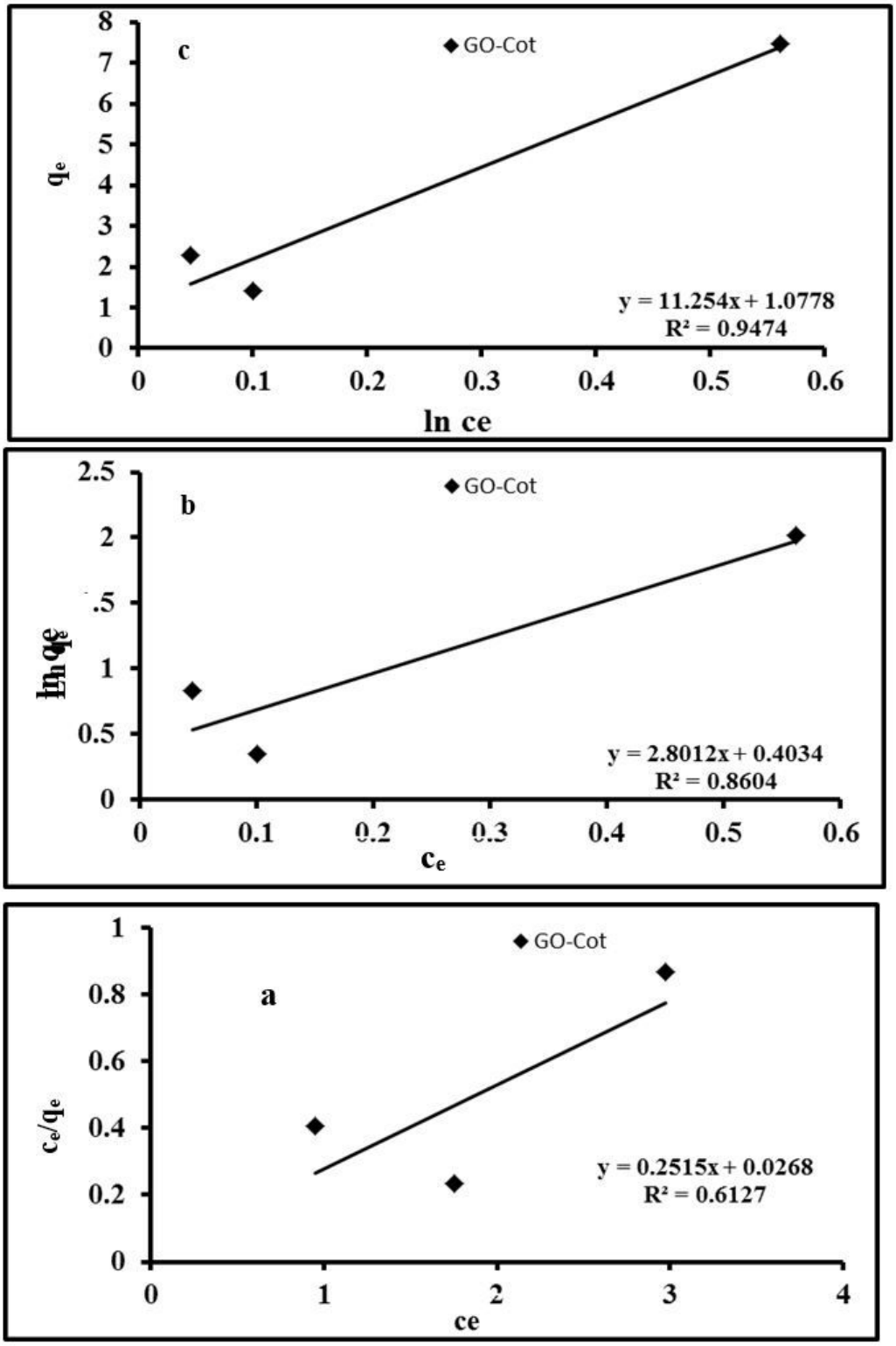

Figure 7

a) Langmuir, b) Freundlich, and c) Temkin isotherm Models Plots for the adsorption of MB dye on GO-Cot, with Optimum Conditions: MB dye concentration (5 mg/L), fabrics (2 × 3 cm), Contact Time 15 Minutes and pH = 9 and T = 298 K.

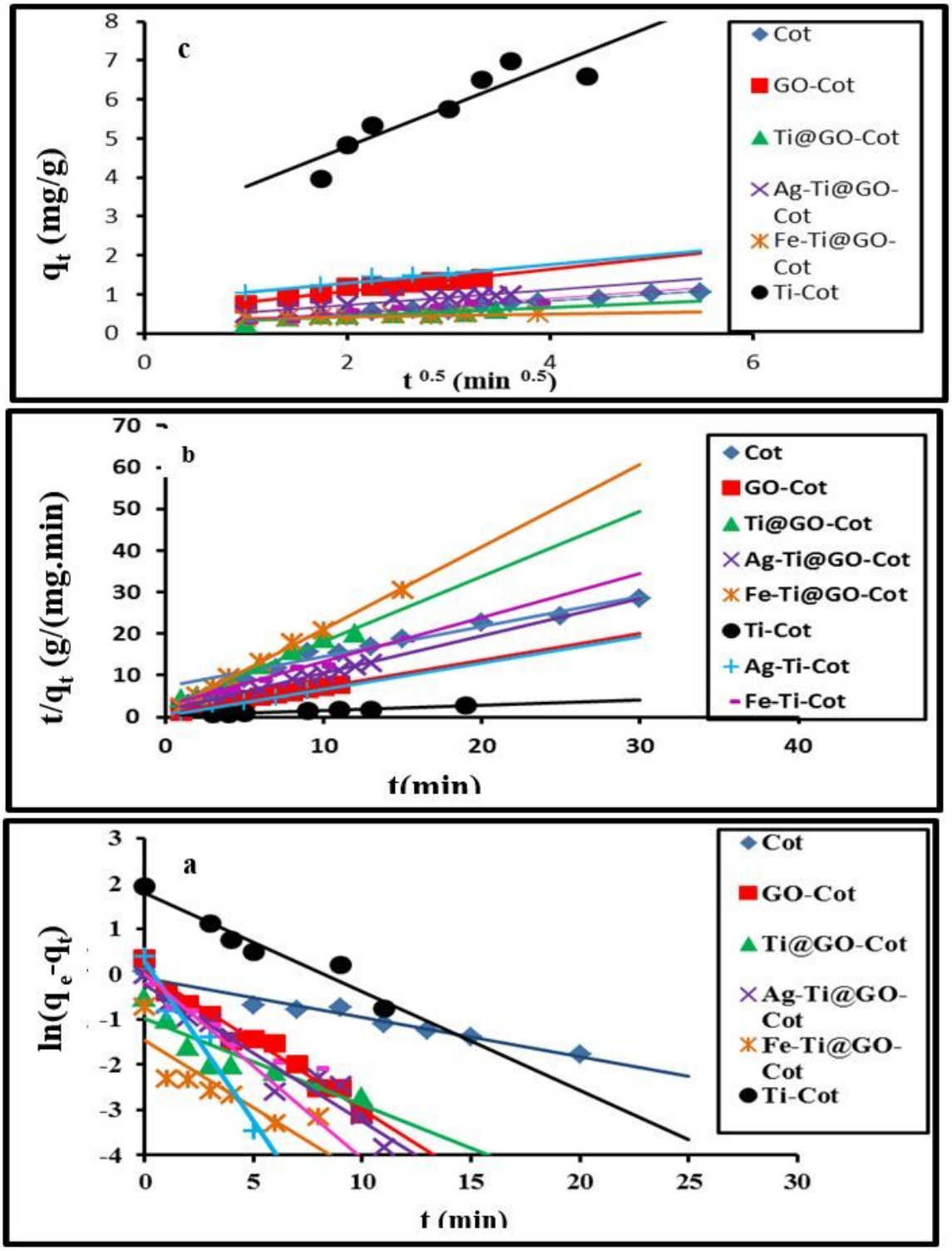

Figure 8

a) Pseudo-first-order b) Pseudo-second-order c) Intraparticle diffusion plots for the adsorption of MB onto cotton and coated cotton samples (with Optimum Conditions: MB dye concentration (5 mg/L), fabrics (2 x 3 cm), Contact Time 15 Minutes and pH = 9 and T = 298 K.

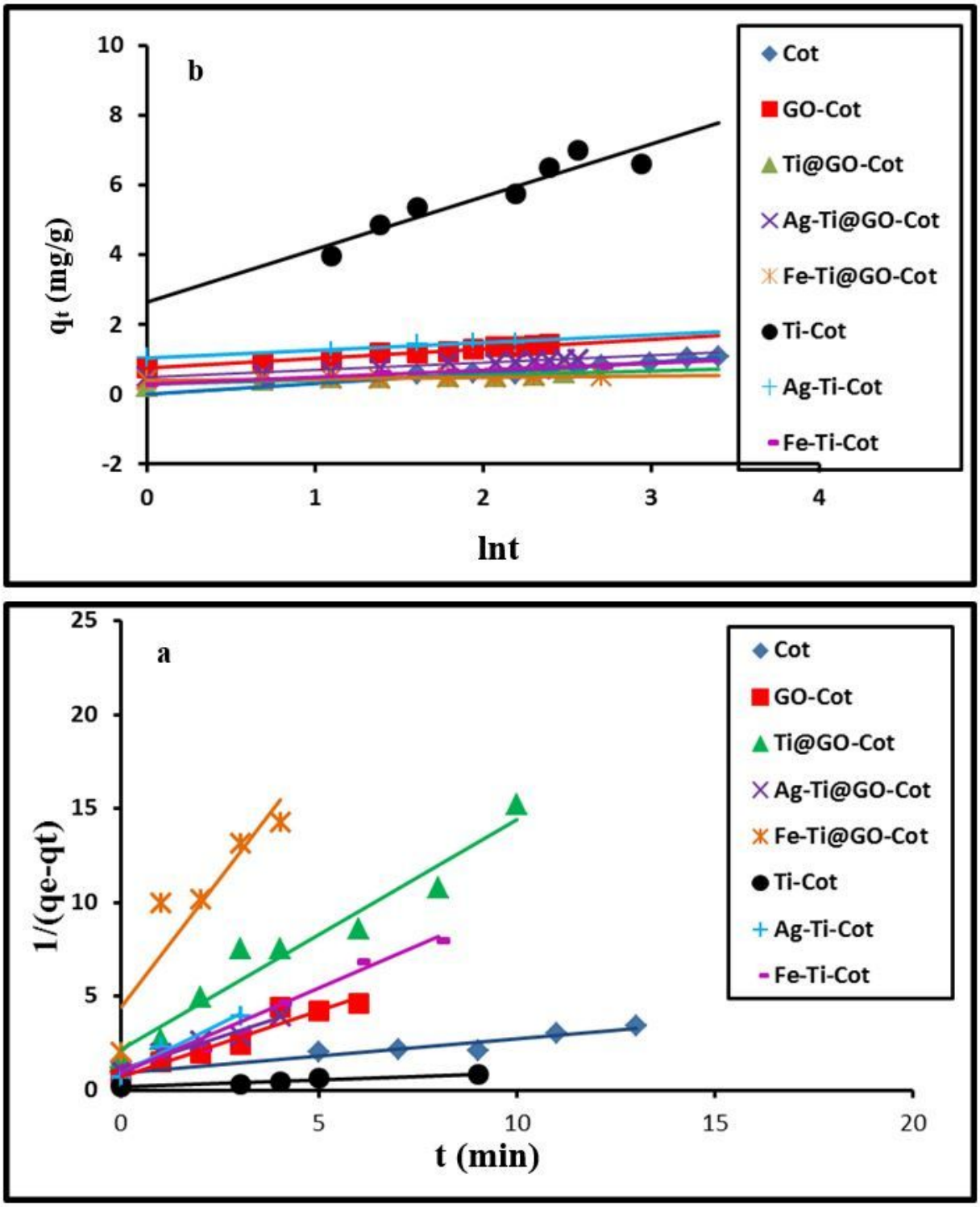

Figure 9

a) Second order model b) Elovich model plot for the adsorption of MB onto cotton and coated cotton samples with optimum conditions: MB dye concentration (5 mg/L), fabrics (2 × 3 cm), contact time 15 minutes and pH = 9 and T = 298 K.